A test of ground-penetrating radar for detecting vertebrate fossils at Tule Springs Fossil Beds National Monument, Nevada

Thomas M. Urban, September 2022

tmurban@geotechglobal.org

Citation:
Urban, T.M. 2022. **A** test of ground-penetrating radar for detecting vertebrate fossils at Tule Springs Fossil Beds National Monument, Nevada. *Geotech Global Consulting Technical Report: TR-1978.*

Key Findings:

- Ground-penetrating radar detected anomalies at seven test sites in Tule Springs Fossil Beds National Monument that may be related to the presence of vertebrate fossils.
- Some of the anomalies are highly suggestive of vertebrate skeletal elements.
- The method was effective on both horizontal and vertical surfaces for the full depth-range of interest.
- Each test location required less than twenty minutes to complete data collection.

1. Background:

On September 8th and 9th, 2022, a pilot study was undertaken at Tule Springs Fossil Beds National Monument (TUSK) to test the efficacy of ground-penetrating radar (GPR) for the in-field detection of Pleistocene vertebrate fossil deposits found within the Las Vegas formation. These fossils are known to be abundant throughout the area (Springer et al. 2017; 2018) and have been the subject of field investigation for decades (e.g., Haynes 1967). The study was proposed by the National Park Service (NPS), funded by NV Energy as part of the Greenlink West project, and undertaken by Thomas Urban, Geotech Global Consulting, as a sub-contractor of Logan Simpson. The geophysical fieldwork (data collection with GPR) was conducted by Urban in collaboration with NPS and U.S. Geological Survey (USGS). personnel. Participants included USGS geologists Kathleen Springer and Jeff Pigati, NPS senior paleontologist Vincent Santucci, TUSK personnel Jeff Axel (acting superintendent), Erin Eichenberg, Lauren Parry, and Aubrey Bonde, and White Sands N.P. personnel David Bustos and Patrick Martinez. Data processing and analysis was conducted by Urban in the week following the fieldwork.

GPR and other geophysical imaging techniques have seen widespread use in archaeology in recent decades, though only very limited use in paleontology. While geophysical methods have been used successfully for detecting the skeletal remains of a wooly mammoth in a frozen tundra lake at Bering Land Bridge National Preserve, Alaska, (Urban et al. 2016) and for detecting trace fossils of Pleistocene megafauna at White Sands National Park, New Mexico, (Urban et al. 2018; 2019), each context is unique. It was therefore unknown whether GPR would be successful in detecting fossils at TUSK.

In addition to the primary question of whether fossils could be detected at all, related questions emerged:

1. If fossils could be detected with GPR, how deep could they be detected?
2. Could fossils be detected in areas where only a vertical survey surface was accessible?
3. Could fossils be detected in carbonate-capped deposits, or would attenuation of the signal be too great?
4. If fossils were detected, what size fossil could be resolved? And the related question, could any meaningful level of detail be resolved on detected fossils?
5. Could fossils be identified in radargrams (B-scan) or would 3-D imaging be required?

Test sites were selected with these questions in mind, to test a range of scenarios. As an experimental project, the scope was limited to seven test locations determined in coordination with NPS and USGS personnel. Sites are described below, separated by those that are in the Greenlink West Right of Way (ROW) and those at other locations within the park boundaries. The collection order of each test is given in parentheses at the end of the description (e.g., Day 1, Test Site 1), and a photo of each test location is included below (Figures 1 – 7).

A. Greenlink sites tested from east to west:

1. Bed E1a or E1b of the Las Vegas Formation (LVF) - GPR across the top of a notable stacked outcrop that contains multiple beds of the LVF. This site was a test of depth capability ((b) (3)
2. Across the top of bed D2 of the Las Vegas Formation (beds D2 and D3 are the highest groundwater events in the LVF and are both marsh ecosystems). Age range of bed D2 is 31.73-27.56 ka. This site was a test of penetration in carbonate-capped deposits with likely higher attenuation ((b) (3))
3. Across the top of bed D3 of the LVF. Age range of bed D3 is 25.86 - 24.43 ka. (b) (3))

B. Other sites tested:

1. (b) (3) Multiple beds of the LVF. GPR concentrated on the YD portion of the section, bed E2a of the LVF. Two dates at this site: 12.85 ka and 12.9 ka. This was the only test of a vertical survey surface. ((b) (3))
2. (b) (3) bed E1b of the LVF; ~14.5 ka ((b) (3))
3. (b) (3) two tusk site; bed E0 of the LVF. Dated site 21.31 ka ((b) (3))
4. (b) (3) bed E0 of LVF; ~19.5 ka. (b) (3))

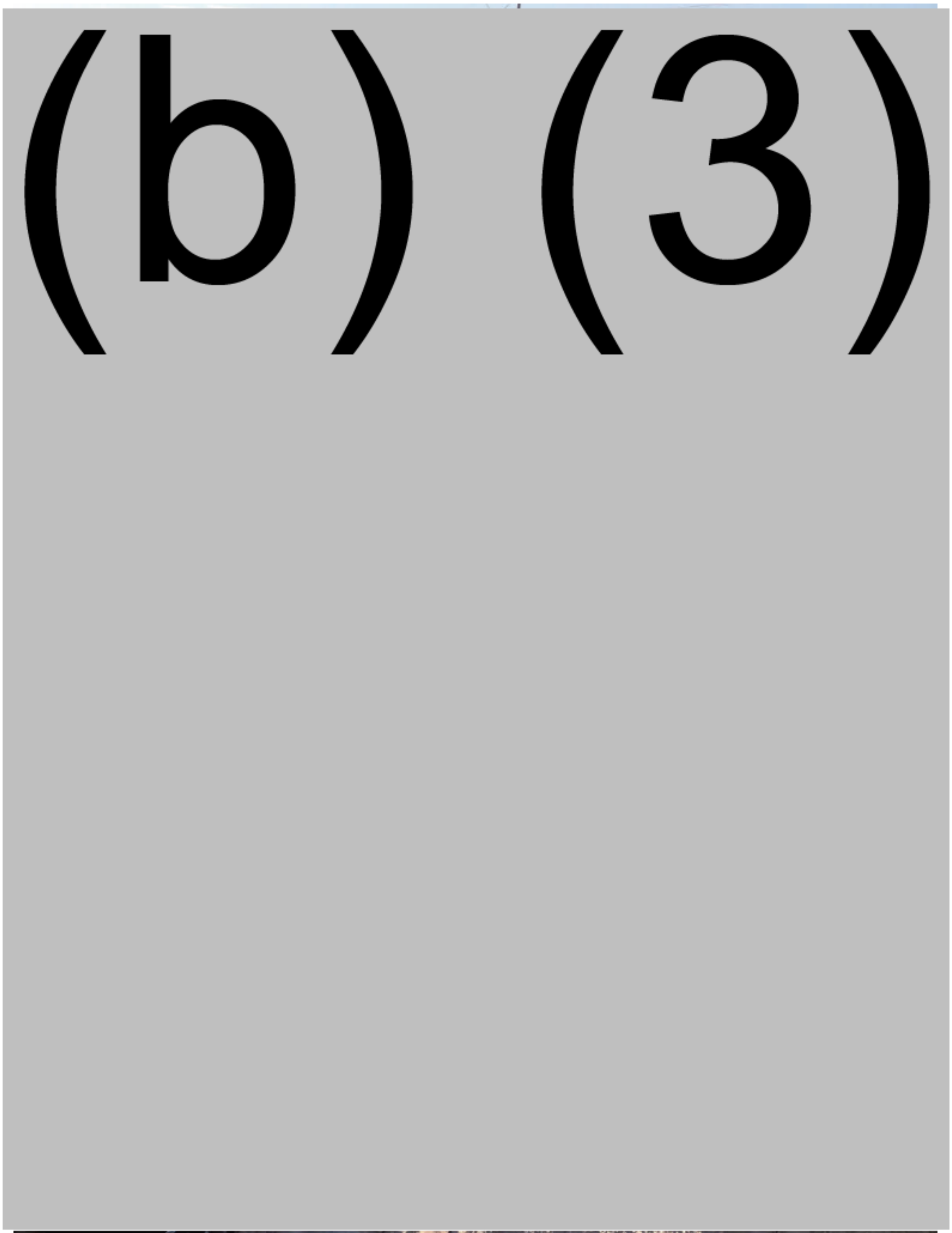

Figure 1. (b) (3)

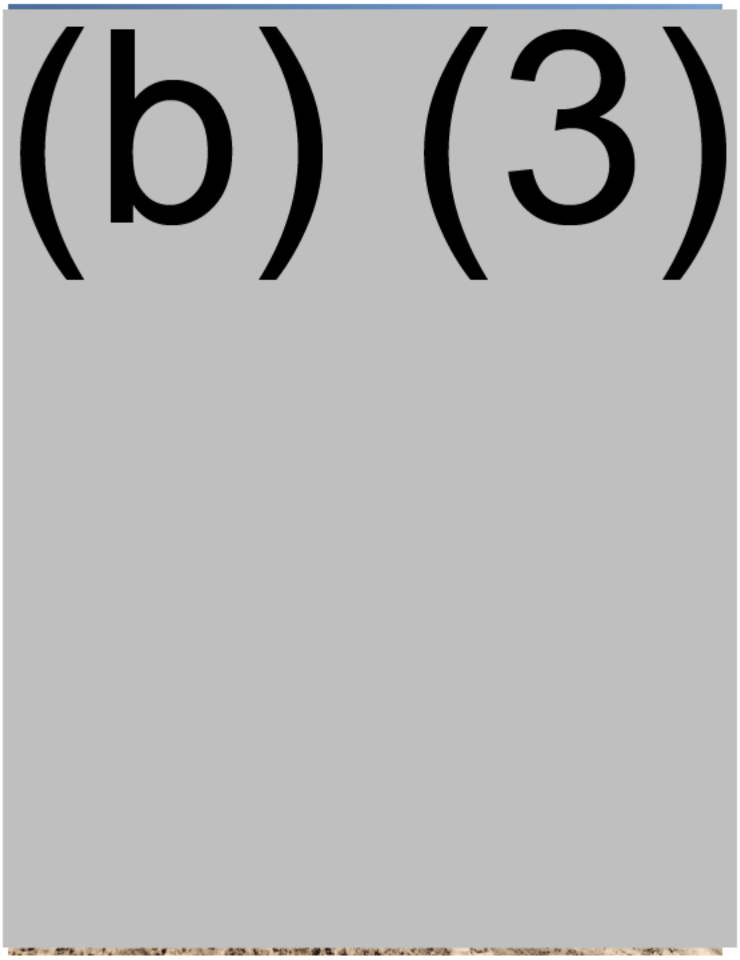

Figure 2. (b) (3)

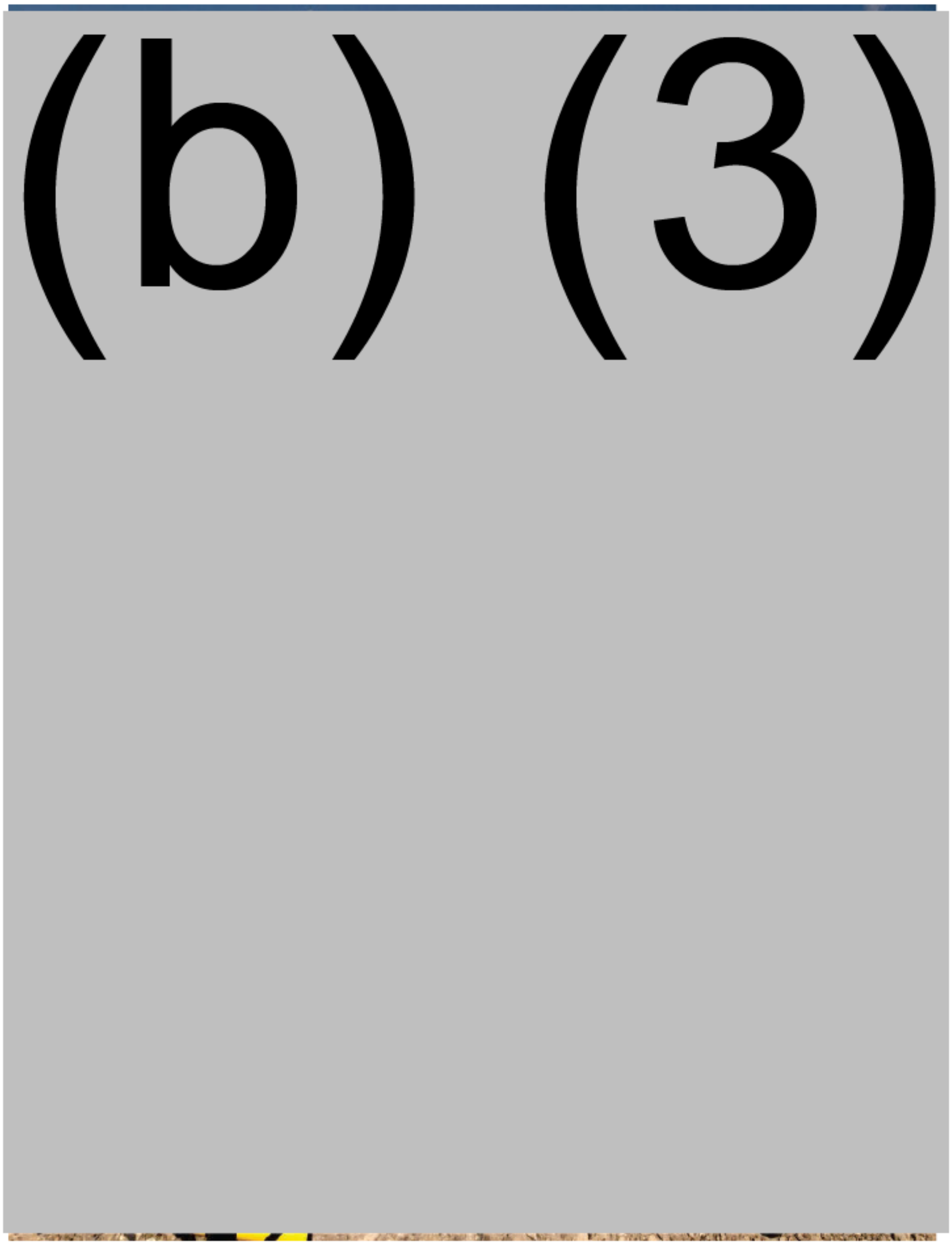

Figure 3. (b) (3)

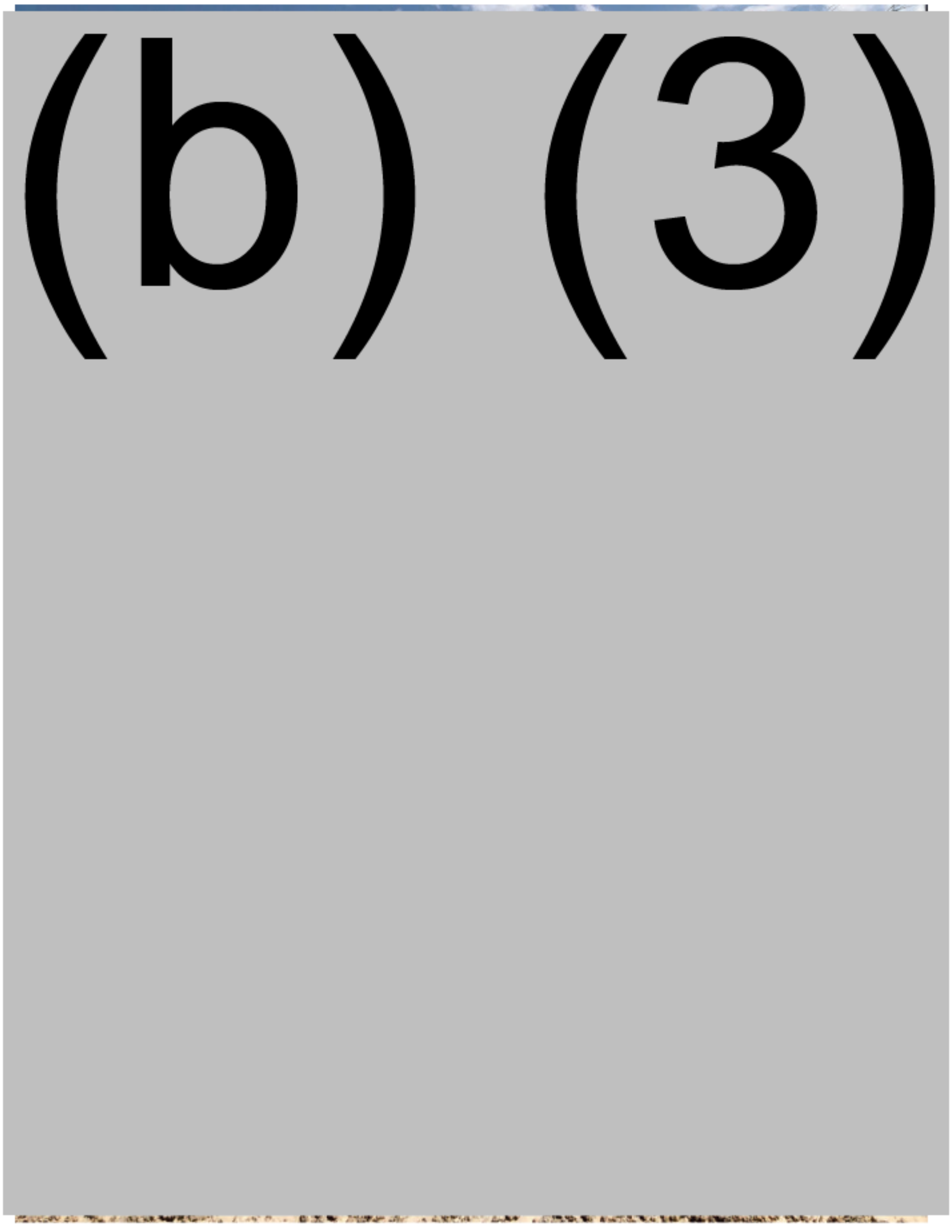

Figure 4. (b) (3)

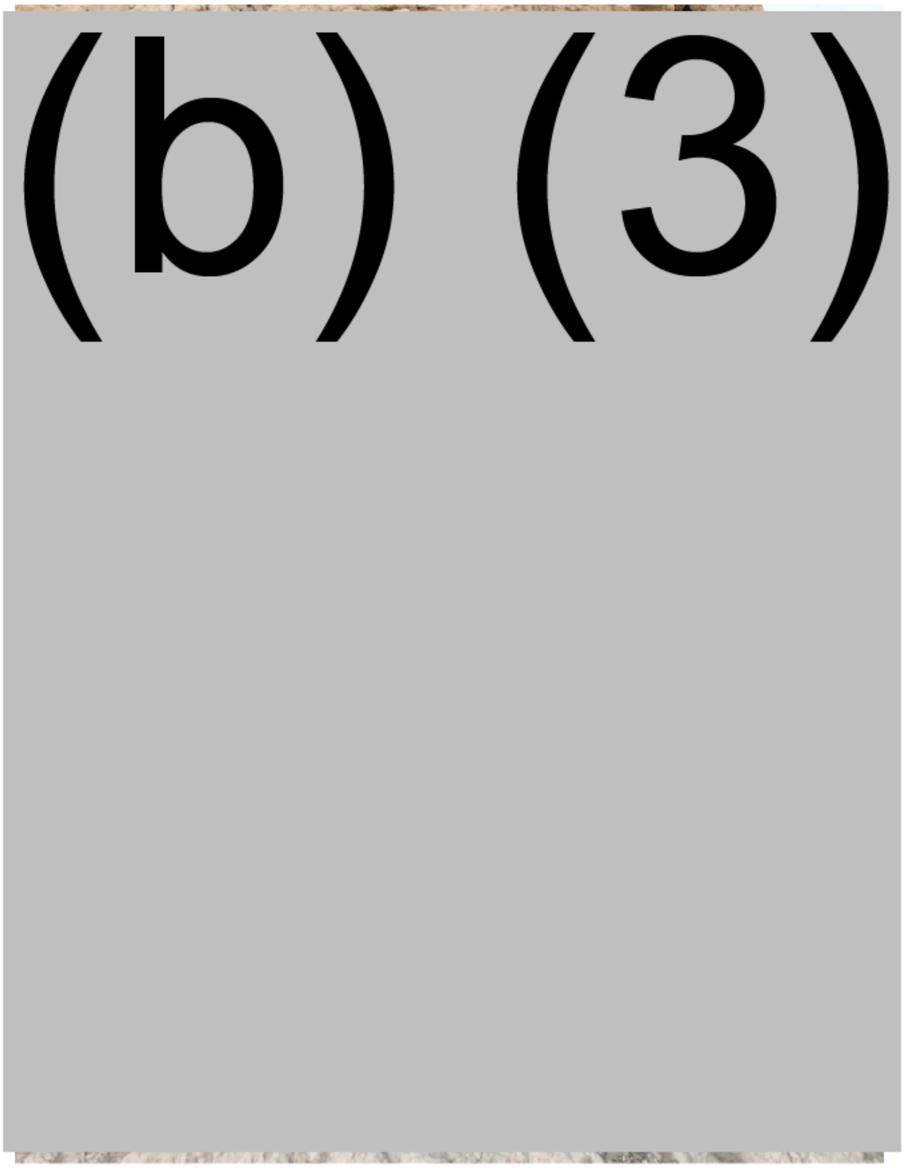

Figure 5. (b) (3)

(b) (3)

Figure 6. (b) (3)

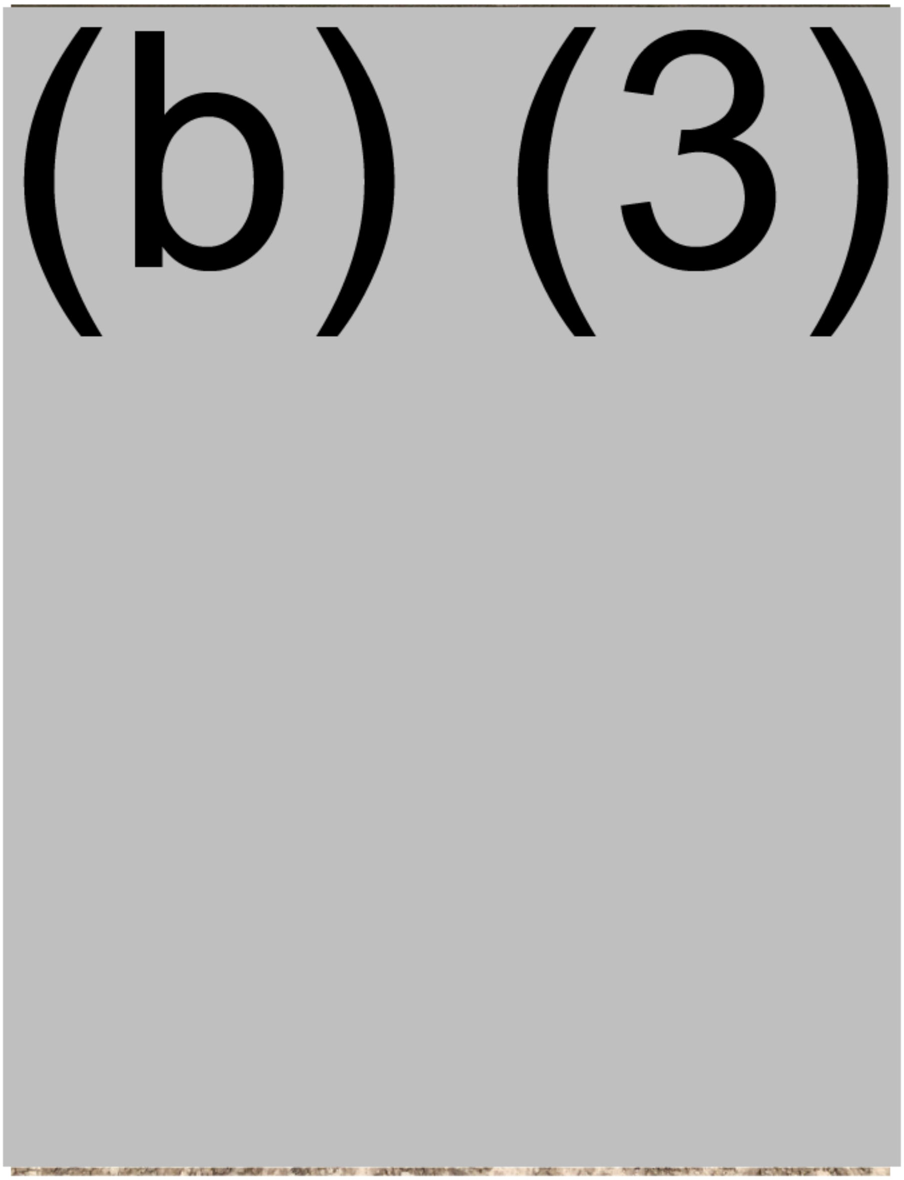

Figure 7. (b) (3)

2. Methods:

A Noggin 250 MHz center frequency, pulsed GPR system by Sensors and Software Inc. was deployed on a sled configuration. System settings varied by test location (Table 1.). Notably, (b) (3) used a longer time window to "see" deeper given the thickness of the deposits in question, and (b) (3) used timed interval transmitting of the pulse due to the difficulty of using the odometer wheel on a vertical surface. Survey parameters also varied by location to accommodate the unique geometry of each test site (Table 2.)

Test Site	Trigger method	Trace interval	Time Window	Stacks
1	odometer	5 cm	124 ns	8
2	odometer	5 cm	124 ns	8
3	odometer	5 cm	124 ns	8
4	odometer	5 cm	374 ns	8
5	timed interval	0.1 s	124 ns	8
6	odometer	5 cm	124 ns	8
7	odometer	5 cm	124 ns	8

Table 1. System settings by site.

Test Site	Survey type	Line spacing (cm)	Line orientation	# of lines	Line length (m)
1	For/Rev	50	N-S and E-W	6	5-10
2	For/Rev	25	E-W	5	15
3	For/Rev	25	E-W	4	10
4	For/Rev	50	E-W	2	32
5	For/Rev	10	E-W	8	1
6	For/Rev	25	E-W	11	4
7	For/Rev	25	N-S	10	4

Table 2. Survey parameters by site.

Processing for the 3-D data included – dewow (remove avg. of values down-trace), background average subtraction (remove avg. of values across multiple traces to remove or suppress flat-lying events), Stolte migration (collapses hyperbola tails), instantaneous amplitude (eliminates phase, envelopes the trace), and amplitude equalization gain (compensates for energy loss with depth and attenuation). 3-D volumes were created as HDF files and figures produced as rendered volumes with partial opacity, iso-surfaces (surfaces of continuous amplitude), oblique planes (i.e., slices), or some combination thereof. In some cases, an additional low pass filter (3-D spherical averaging) or high pass filter (Laplacian) were applied if warranted to improve image quality. Velocity was estimated to vary between 10 and 12 cm/ns, using the hyperbola fitting method, and this was used for time-depth conversion and migration. For limitations on velocity estimation see Jacob and Urban 2015.

Processing for radargrams included dewow, SEC-2 gain (Spreading & Exponential Calibrated Compensation), total background average subtraction (to eliminate direct waves), and in some cases attribute analysis in the form of the Instantaneous phase (eliminates amplitude and enhances continuous events), and band pass filter (to narrow the frequency band, enhancing certain events).

3. Results

(b) (3)

Profiles collected at the (b) (3) exhibited a number of sub-surface anomalies which could be related to the presence of fossils (Figure 8-9). Multiple horizons were also evident in the data. The resulting radargrams are comparable to what the GPR operator observes live on screen while collecting the data. This is the most basic ways to present GPR data with minimal processing. If fossils could be positively identified with only the radargram, this would be the fastest approach. As this site is slated for later excavation, there will be a basis for comparison.

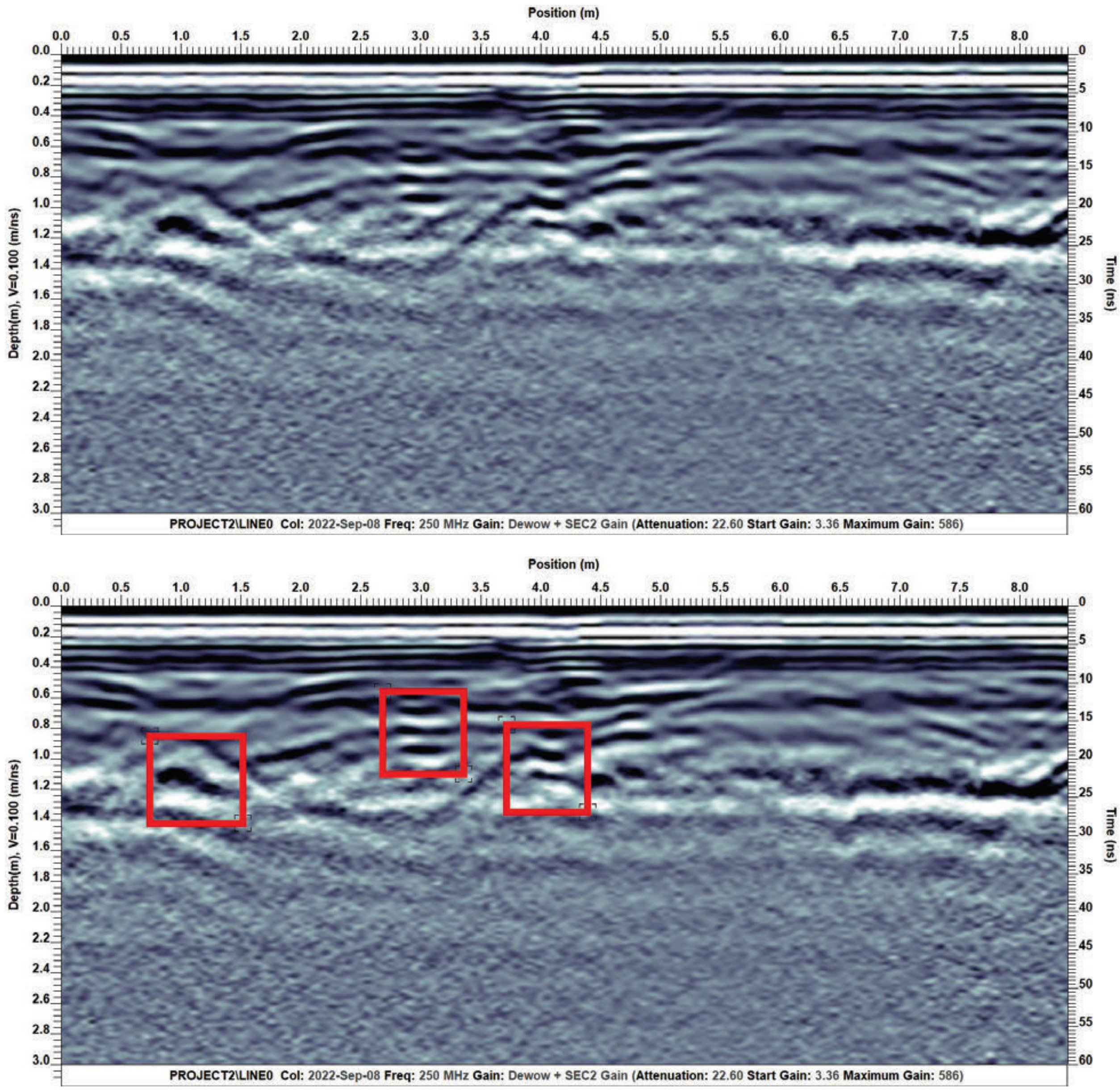

Figure 8. Top: radargram at the (b) (3) exhibit various horizons as well as discrete anomalies. Bottom: several discrete anomalies indicated with red boxes could be caused by fossils.

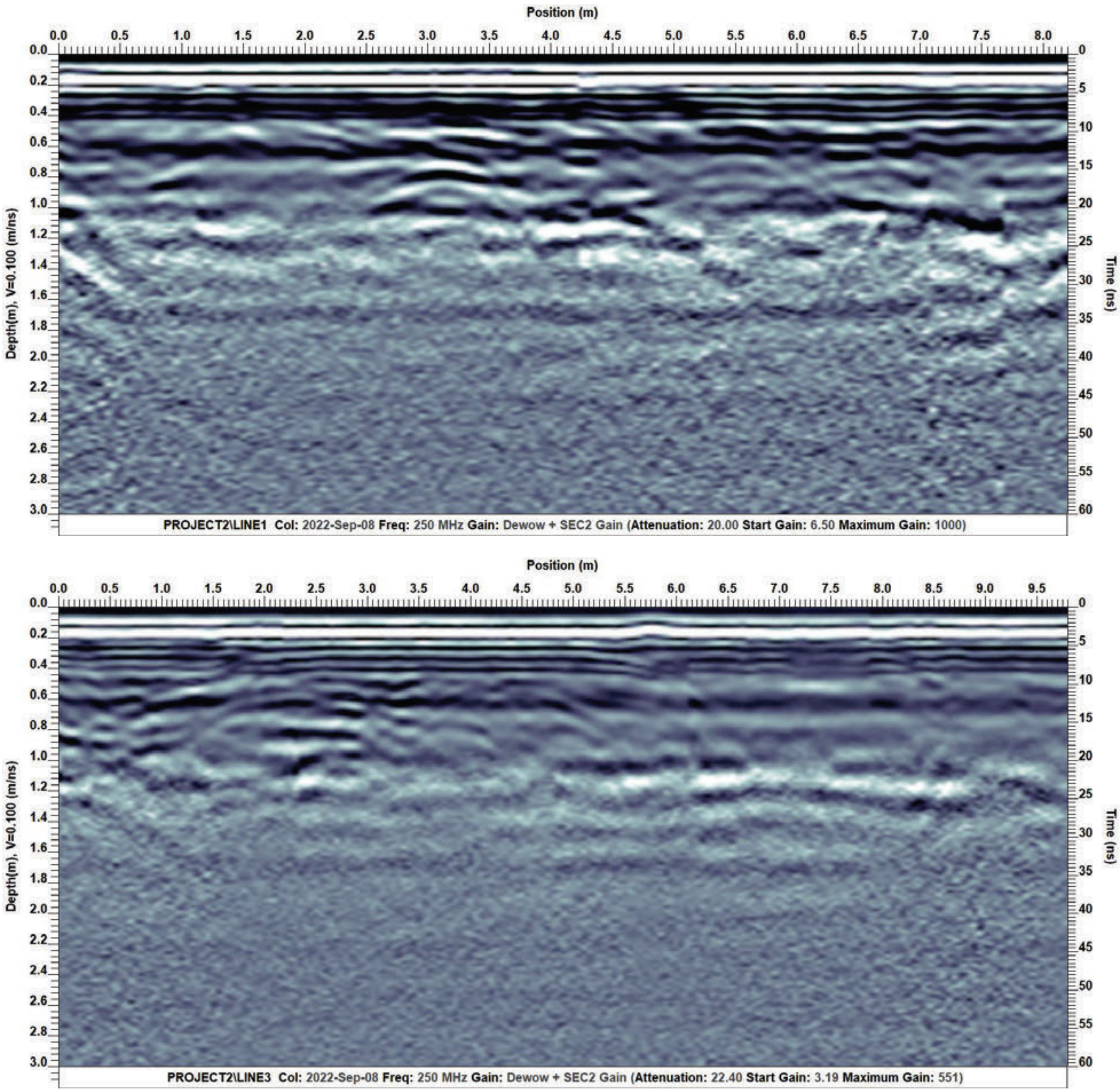

Figure 9. Two more examples of radargrams from the (b) (3) , with each exhibiting various anomalies in the sub-surface.

(b) (3)

This narrow 3-D grid collected across the top an outcropping exhibited a collection of anomalies that could well be vertebrate fossils. A cluttered assemblage of these anomalies was more concentrated toward one half of the survey grid (Figure 10).

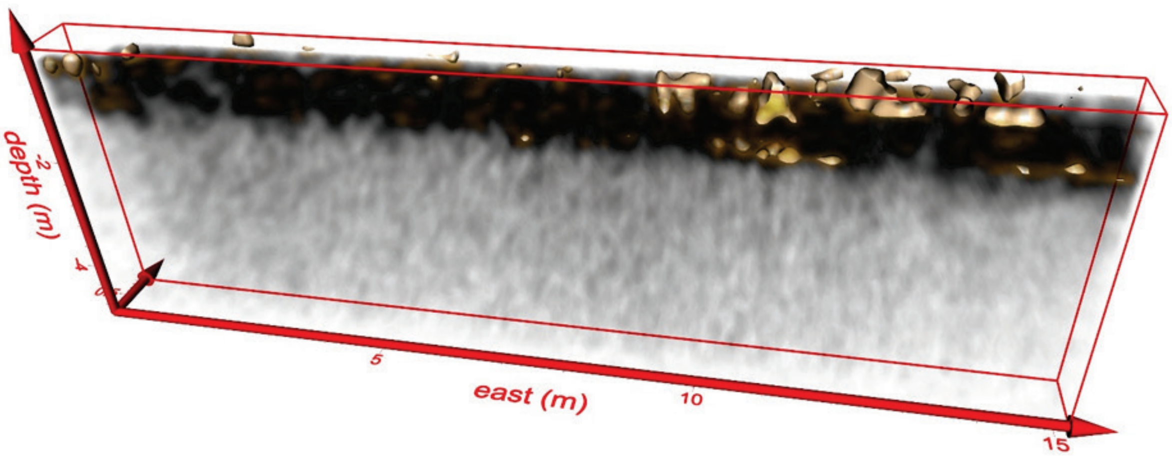

Figure 10. (b) (3) This test was conducted by collecting GPR data atop an outcrop of several meters height. The upper meter contained some anomalies, with a particular concentration from 8-14 m (right side in the above image). The figure combines a partially opaque rendered volume with an isosurface. The data were dewowed, gained, background filtered, migrated and enveloped.

(b) (3)

The small ground-level grid collected at (b) (3) exhibited several anomalies which were more apparent in the radargram with the application of the instantaneous phase, perhaps because the ground-level survey exhibited greater attenuation (Figure 11). Notably, a large anomaly was apparent between 9-10 meters along the long axis of the grid, and extending to a depth of nearly 2 m. When processed for 3-D rendering, the anomaly exhibited scale and shape reminiscent of a proboscidean skull, while another anomaly centered at 4 m along the grid axis and approximately 1 m deep, exhibited form similar to a long bone (Figure 12).

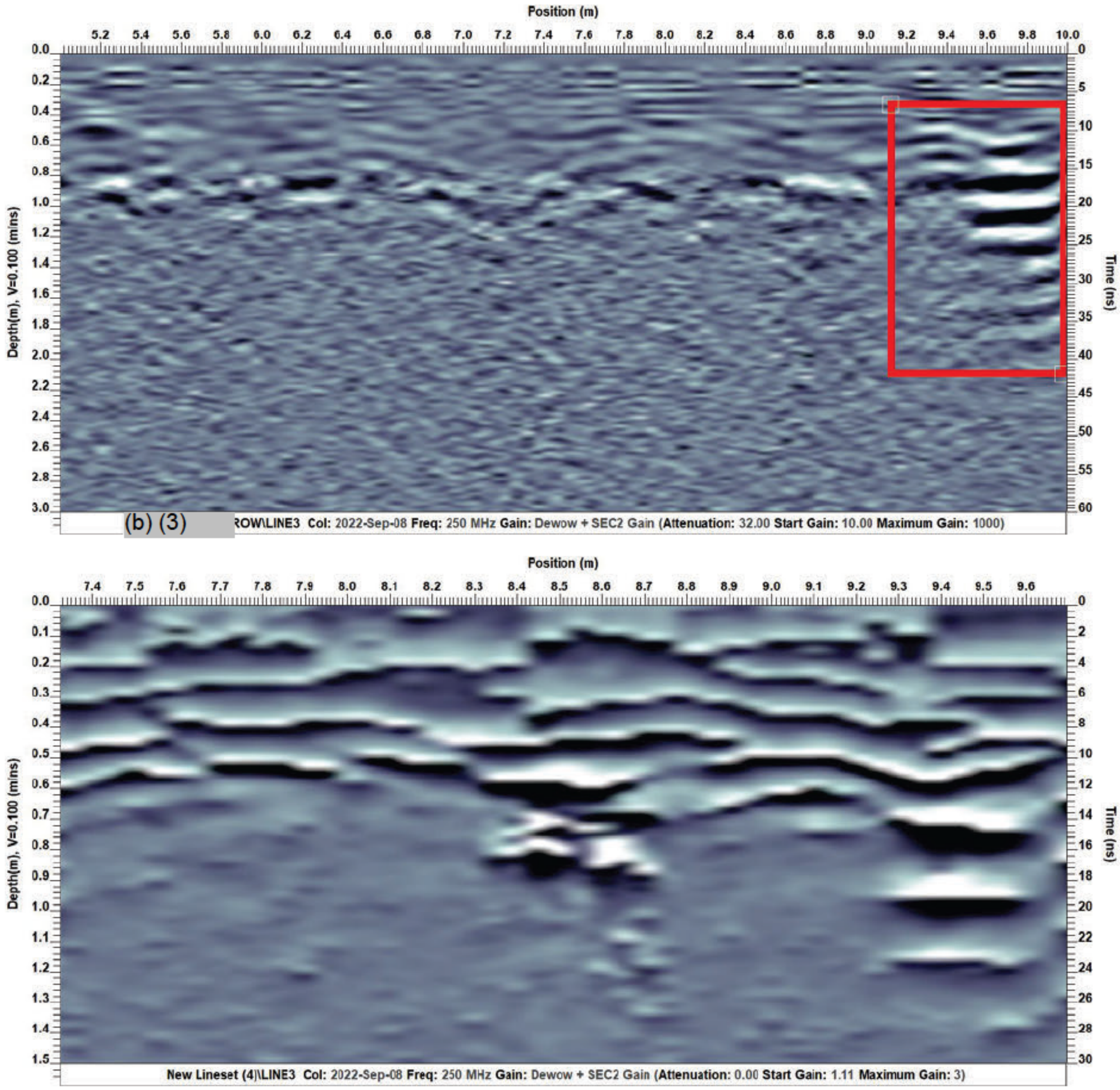

Figure 11. Top: radargram from (b) (3) with red box indication a large anomaly at one end of the survey. Bottom: Instantaneous phase applied to the same radargram and zooming in on the location of the large anomaly.

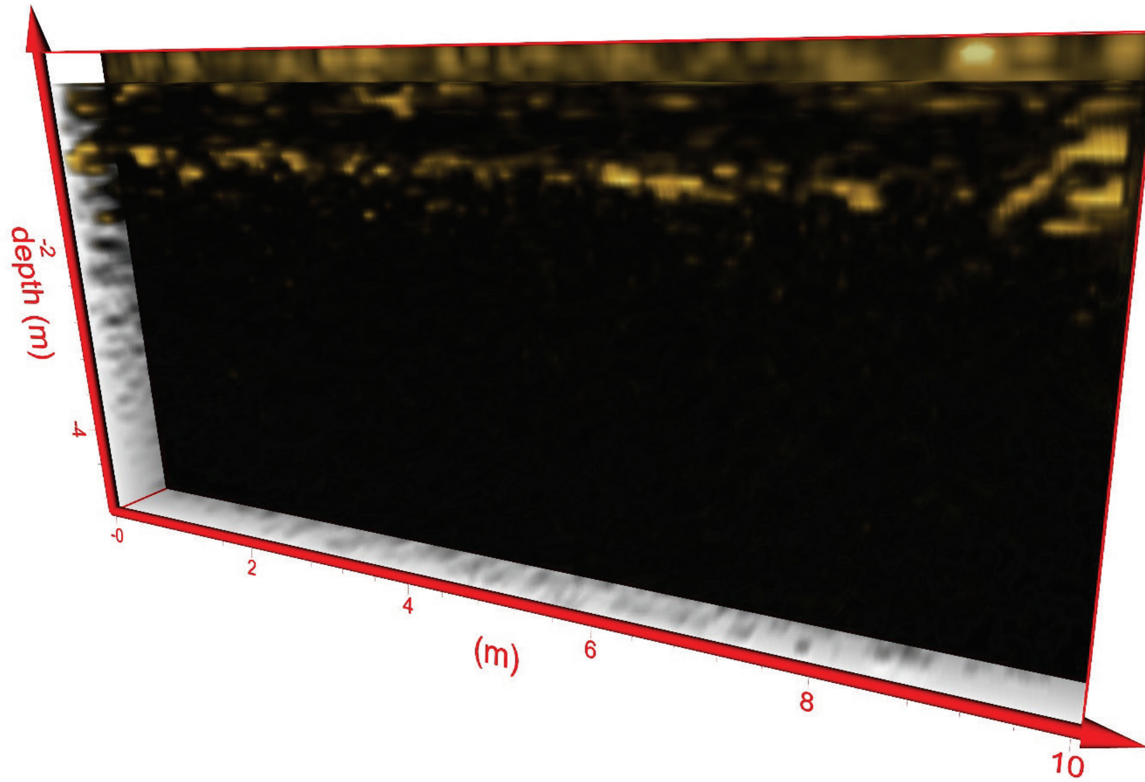

Figure 12. (b) (3) This location tested open-ground carbonate capped substrate and exhibited notable higher attenuation of the signal (possibly related to recent precipitation). The upper meter contained some notable anomalies, the largest of which occurred at 9-10 m (upper right in above figure). This particular anomaly measures approximately 1m in all dimensions (d, w, h). The figure combines a partially opaque rendered with an oblique image. The data were dewowed, gained, background filtered, migrated and enveloped, and high pass filtered.

(b) (3) .

(b) (3) the deepest test, included two anti-parallel profiles across the top of a stacked outcrop. This was the deepest test conducted, with a time-window that corresponded to a depth of 15m or more. The survey appeared to detect anomalies for the full depth range (Figure 13).

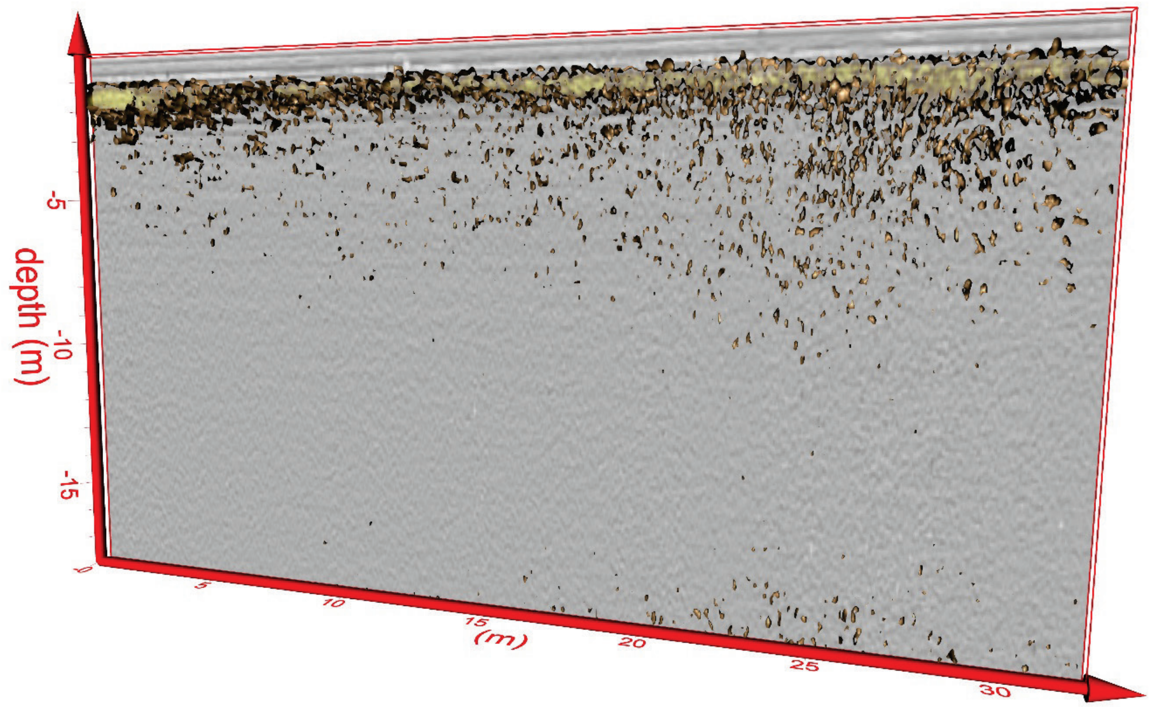

Figure 13. The image combines a bandpass filtered, partially opaque radargram with rendered volume and isosurface. Numerous anomalies were detected throughout the sampled depth range.

(b) (3)

(b) (3) was the only test of a vertical surface. The small test, conducted at (b) (3) required the instrument to be reconfigured and also required assistance with data collection (one person controlling the instrument console with two others moving the antenna across the vertical surface). An anomaly was detected between 1 and 2 m into the wall, though it is unknow whether the anomaly is related to a fossil (Figure 14).

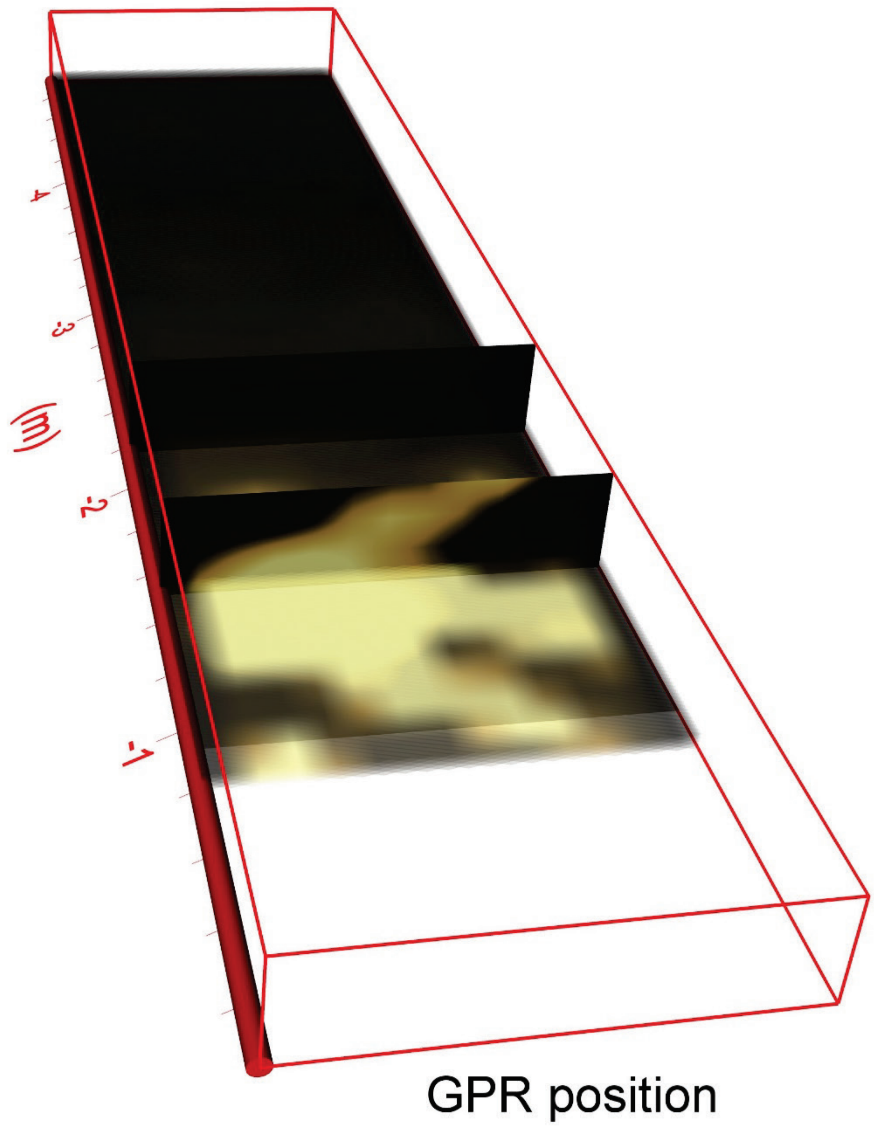

Figure 14 (b) (3) . This survey, conducted at (b) (3) tested the capability of detecting fossils through a vertical survey surface. To do so, the radar antenna was rotated to match the surface, and the trigger method was switch from odometer to timed sampling. Deployment of the system in this configuration required assistance (as opposed to single-operator deployment on horizontal surfaces). An obvious anomaly was detected between 1 and 2 m into the vertical surface. The figure combines a rendered volume with two oblique images. The data were dewowed, gained, background filtered, migrated and enveloped.

(b) (3)

This small grid was placed across the top of a deposit with a large concentration of visible eroding bone fragments. Anomalies similar to those seen at the other test location were visible in the radargrams (Figure 15). The 3-D rendering of the data yielded a result very suggestive of larger vertebrate fossils in the sub-surface beneath the visible bone fragments. The form of the anomalies bares close resemblance to skeletal material (Figure 16).

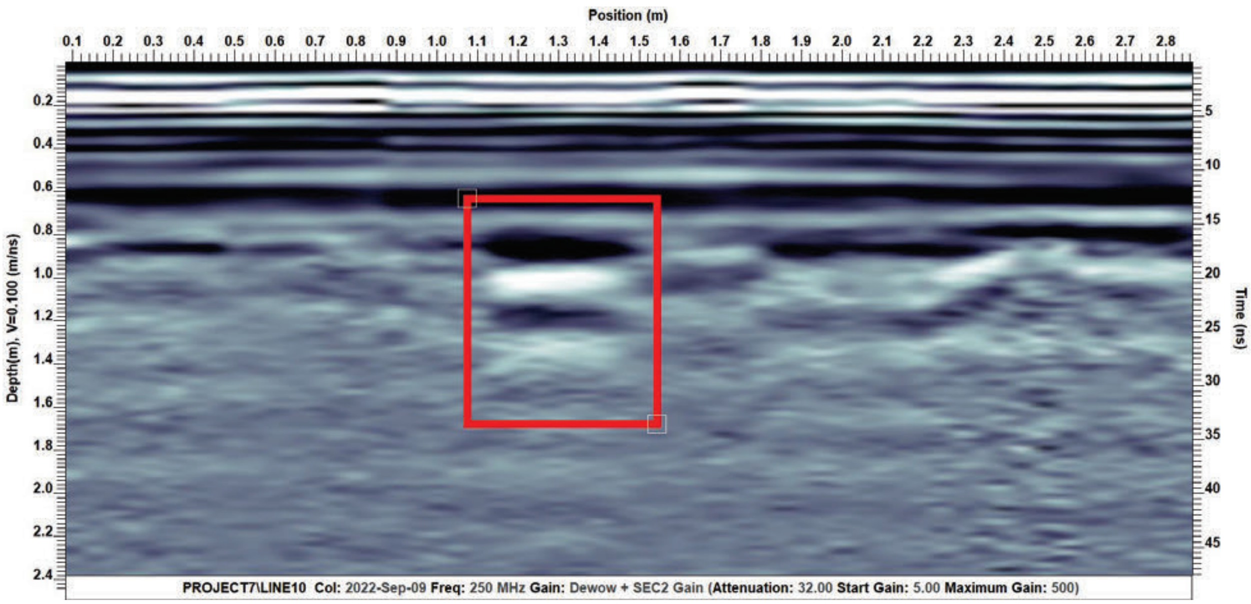

Figure 15. Radargram from (b) (3) with red box indicating an anomaly.

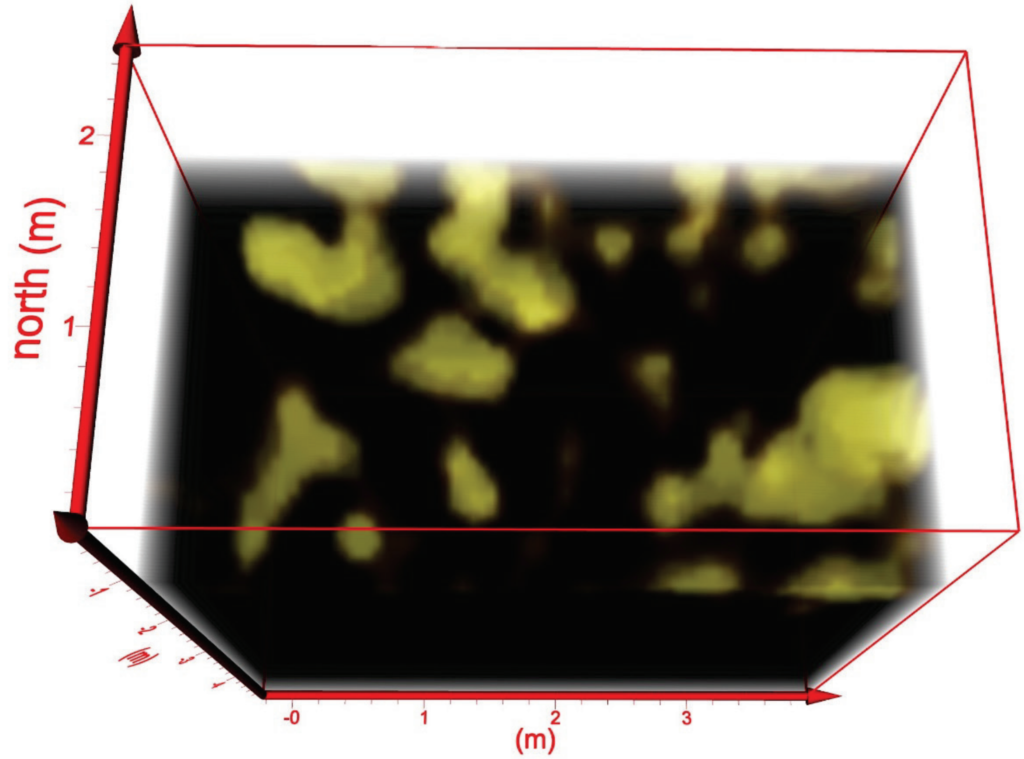

Figure 16. (b) (3) This survey was conducted on deposites that exhibited a large amount of small bone fragments eroding out of the surface. A number of anomalies were detected, some of which resemble vertebrate fossils as shown here. In the above figure, a rendered volume was sliced using a clip-plane to a depth of approximately 1 m. The data were dewowed, gained, background filtered, migrated and enveloped.

(b) (3)

This small grid was collected on a flat surface at the top of a slope down into a wash. Two visible mammoth tusks were protruding from the slope approximately 1-1.5 m below the survey surface. The radargrams exhibited several prominent anomalies (Figure 17). As with the previous test, 3-D rendering provided a more compelling result, with the form of anomalies closely resembling skeletal material (Figure 18).

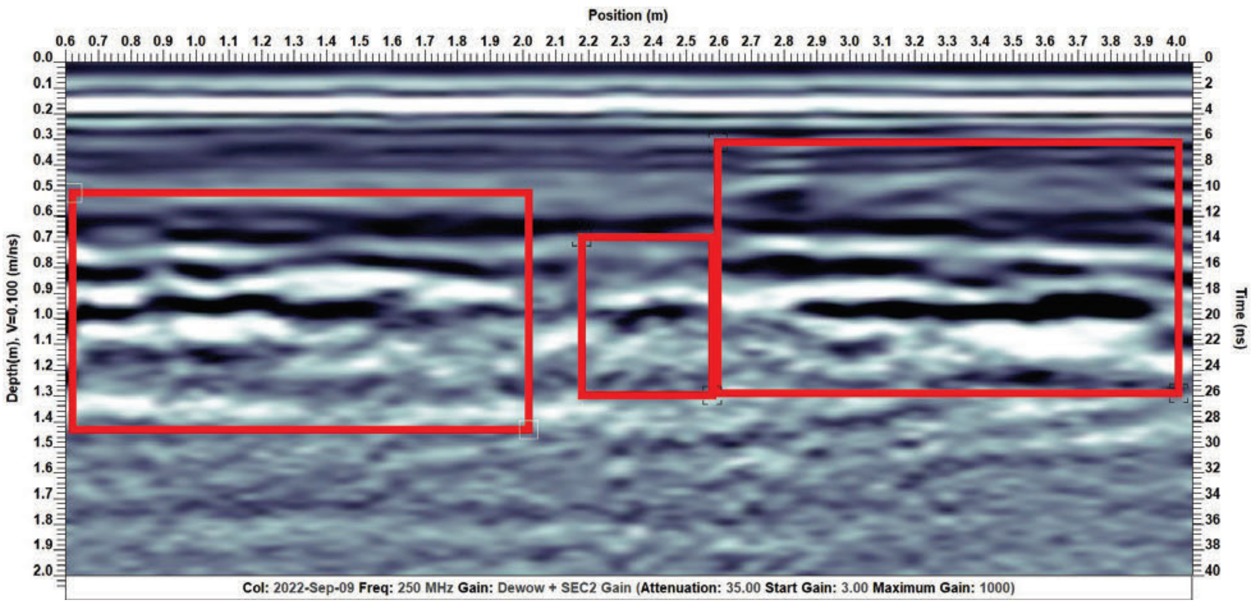

Figure 17. A sample radargram from the (b) (3) site survey with red boxes indicating several anomalies.

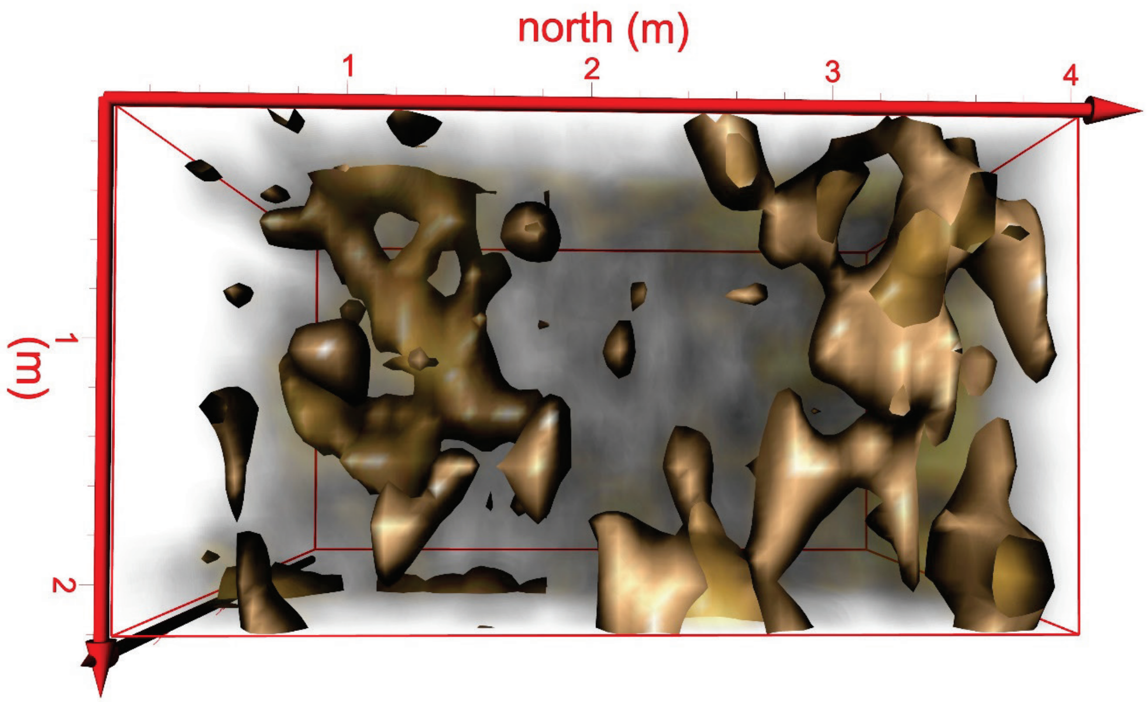

Tusks visible here

Figure 18: The (b) (3) site exhibited two proboscidean tusks protruding from an escarpment. GPR data was collected from above. In the figure, a top-down view is used, looking down through a partially opaque ground. A number of anomalies detected in the depth range of the tusks are strikingly reminiscent of proboscidean skeletal remains. The figure was made by combining an isosurface of continuous amplitude with a partially opaque rendered volume. The data were dewowed, gained, background filtered, migrated and enveloped.

4. Conclusions and Recommendations:

The primary question of the pilot study concerned whether GPR is capable of detecting vertebrae fossils at TUSK. The tests at TUSK detected anomalies in seven representative field scenarios, including in deposits deemed to have a high likelihood of vertebrate fossil presence. Further, many of the detected anomalies exhibited forms highly suggestive of vertebrate skeletal elements. Barring alternative explanations for these anomalies, the most reasonable explanation is that they are likely caused by the presence of fossils. Some related questions were also addressed:

Q1. If fossils could be detected with GPR, how deep could they be detected?

A1. In the deepest test case, anomalies were detected at depths greater than 10 meters.

Q2. Could fossils be detected in areas where only a vertical survey surface was accessible?

A2. Yes, the method was successfully deployed on a vertical surface.

Q3. Could fossils be detected in carbonate-capped deposits, or would attenuation of the signal be too great?

A3. Yes, this appeared to make little difference.

Q4. If fossils were detected, what size fossil could be resolved? And the related question, could any meaningful level of detail be resolved on detected fossils?

A4. This is a difficult question to address without ground-truthed results. It appears that meaningful detail was resolved, though several measures could be taken to improve resolution (described below).

Q5. Could fossils be identified in radargrams (B-scan) or would 3-D imaging be required?

A5. Potentially. The anomalies are visible in the radargrams, though interpreting these as fossils from the radargram alone could prove difficult. More compelling results were yielded by 3-D imaging.

Spatial resolution with GPR is related primarily to antenna frequency, sampling intervals, and the electrical properties of the substrate and targets. For a detailed discussion see Urban et al. 2014a, b. In instances where greater detail may be sought, the approach taken here could be adapted to improve resolution by incorporating higher antenna frequencies and/or using higher spatial resolution in the data collection (e.g., more closely spaced lines, smaller trace interval). This would, however, increase data collection time and likely reduce penetration depth.

GPR could easily be incorporated into broader field sampling either as a course reconnaissance method (e.g., long passes looking to flag general disturbances in radargrams) or as a targeted method used for fine-grained surveys of high value locations, possibly incorporating multiple antenna frequencies to balance the trade-offs of depth and resolution. As shown in the results of this pilot study, while fossil deposits likely generate visible anomalies in radargrams, these may be harder to distinguish from other things in the subsurface and may therefore increase the likelihood of false positives in comparison to 3-D imaging. However, experience in particular contexts will generally improve the ability to identify sought-after features with minimal processing. This is obviously aided by comparison of GPR data to ground-truthed cases. In other words, though results and efficiency were good in the pilot study, they would likely be improved with more experience applying the method is this specific context.

5. References:

Haynes, C.V. Jr. 1967. Quaternary Geology of the Tule Springs Area, Clark County, Nevada. In Wormington, H.M. and Ellis, D. (eds). Pleistocene Studies is Southern Nevada: [Carson City] Nevada State Museum Anthropological Papers no 13: 15-104.

Jacob, R.W. and T.M. Urban. 2015. Ground-penetrating radar velocity determination and precision estimates using common-mid-point (CMP) collection with hand-picking, semblance analysis, and cross-correlation analysis: a case study and tutorial for archaeologists. *Archaeometry*, 58: 987-1002.

Springer, K.B., Pigati, J.S., and Scott, E. 2017. Vertebrate paleontology, stratigraphy, and paleohydrology of Tule Springs Fossil Beds National Monument, Nevada (USA). *Geology of Intermountain West* 4: 55-98.

Springer, K.B., Pigati, J.S., Manker, C.R., and Mahan, S.A. 2018. The Las Vegas Formation. U.S. Geological Survey Professional Paper 1839, 62 p. https:/doi.org/10.3133/pp1839.

Urban, T.M. M. R. Bennett, D. Bustos, S.W. Manning, S.C. Reynolds, M. Belvedere, D. Odess, V.L. Santucci. 2019 a. 3-D radar imaging unlocks the untapped behavioral and biomechanical archive of Pleistocene ghost tracks. *Scientific Reports*, 9 (1).

Urban, T.M., D. Bustos, S.W. Manning. M. Bennett. 2018. Use of magnetometry for detecting and documenting multi-species Pleistocene megafauna tracks. *Quaternary Science Reviews,* 199: 206 – 213.

Urban, T.M., J. T. Rasic , C. Alix, D. D. Anderson, S.W. Manning, O. K. Mason, A. H. Tremayne and C.B. Wolff. 2016. Frozen: The Potential and Pitfalls of Ground-Penetrating Radar for Archaeology in the Alaskan Arctic. *Remote Sensing,* 8, 1007.

Urban, T.M., S.W. Manning, J.F. Leon, K.D. Fisher. 2014 a. High resolution GPR detection of Late Bronze Age architecture Kalavasos-*Ayios Dhimitrios*, Cyprus. *Journal of Applied Geophysics,* 107: 129 – 136.

Urban, T.M., Y.M. Rowan, M.M. Kersel. 2014 b. Ground-penetrating radar investigations at Marj Rabba, a Chalcolithic site in the lower Galilee of Israel. *Journal of Archaeological Science*, 46: 96 - 106.